Pediatr Blood Cancer 2013;60:2036–2041

Apparent Diffusion Coefficient of Pediatric Cerebellar Tumors: A Biomarker of Tumor Grade?

Andrea Poretti, MD,[1,2] Avner Meoded, MD,[1] Kenneth J. Cohen, MD,[3] Michael A. Grotzer, MD,[4] Eugen Boltshauser, MD,[2] and Thierry A.G.M. Huisman, MD[1]*

Background: The role of diffusion weighted imaging (DWI) to reliably differentiate tumor types and grades in pediatric cerebellar tumors is controversial. We aimed to clarify the discrepancy reported in previous articles. ***Procedures:*** We retrospectively evaluated the apparent diffusion coefficient (ADC) values of the enhancing, solid parts of cerebellar tumors and correlated the absolute tumor ADC values and cerebellar and thalamic ratios with histology in a cohort of children with cerebellar tumors. ***Results:*** Twenty-four children (12 females) were included in the study. The median age at pre-surgical MRI was 10 years (range 29 days–18.5 years). Absolute ADC values (mean 1.49, SD 0.25 vs. 0.63 ± 0.18), cerebellar (2.04 ± 0.33 vs. 0.83 ± 0.25), and thalamic ratio (1.98 ± 0.35 vs. 0.79 ± 0.23) were significantly higher in low- than in high-grade tumors ($P < 0.0001$). Absolute ADC values and cerebellar and thalamic ratios were significantly higher in low-grade astrocytomas than in MBs. Overlap was seen for WHO grade II and III ependymomas. One hundred percent specific cutoff ADC values of $>1.2 \times 10^3$ and $<0.8 \times 10^{-3}$ mm^2/s were established for low- and high-grade tumors. ***Conclusion:*** ADC analysis of the solid, contrast enhancing components of pediatric cerebellar tumors may facilitate differentiation between various tumor histologies. Pediatr Blood Cancer 2013;60: 2036–2041. © 2013 Wiley Periodicals, Inc.

Key words: apparent diffusion coefficient (ADC); cerebellar tumors; children; diffusion weighted imaging (DWI); magnetic resonance imaging (MRI)

INTRODUCTION

Brain tumors are the most prevalent solid tumors in children. Their incidence is 2.97 per 100.000 [1]. In children older than 1 year of age, most tumors are located within the posterior fossa. Overall, infratentorial tumors account for 45–60% of all brain tumors [2]. Pilocytic astrocytomas (PAs), medulloblastomas (MBs), and ependymomas are the most common pediatric cerebellar tumors, high-grade gliomas, atypical teratoid/rhabdoid tumor (ATRT), and choroid plexus papilloma (CPP) of the fourth ventricle are less frequent.

Conventional magnetic resonance imaging (MRI) is essential for diagnosis and evaluation of location, tumor extent, and involved functional centers, but may not reliably differentiate between high- and low-grade tumors and offers limited information regarding tumor type [3]. Advanced MRI techniques have shown to provide important additional information about the biological, physiological, and metabolic features of brain tumors [4]. Recent studies suggested that diffusion weighted imaging (DWI) may effectively distinguish between various cerebral tumor types and histologic grades [5,6]. The role of DWI for differentiation of the pediatric cerebellar tumors has also been evaluated [7–14]. The results of these studies appear however controversial: a variable specificity of ADC values for differentiating cerebellar tumors and an overlap in the apparent diffusion coefficient (ADC) values of various cerebellar tumors types have been reported. In order to resolve this controversy we performed a retrospective study focusing on the solid contrast enhancing component of the cerebellar neoplasms. We evaluated the ADC values of different pediatric cerebellar tumors in a cohort of children with histologically proven cerebellar tumors and aimed to clarify the discrepancy reported in the previous articles.

METHODS

This study was approved by the institutional research ethics board.

Subjects

The inclusion criteria for this study were: (1) a histological confirmed cerebellar neoplasm and (2) the availability of a pre-surgical MR-study including axial T2-, axial fluid-attenuated inversion recovery (FLAIR)-, and axial and sagittal pre- and post-contrast T1-weighted images and DWI images. Eligible patients were collected through an electronic search of our pediatric neuroradiology database covering the time period between January 1st, 2008 and March 31st, 2011.

Diffusion Weighted Imaging

All MRI studies were performed on 1.5 T scanner (Siemens Avanto, Erlangen, Germany). DWI sequences were acquired using a diffusion-weighted single-shot echo-planar sequence with diffusion gradients along the three standard *X*, *Y*, and *Z* directions and effective b-values of 0 and 1,000 s/mm^2. Scan parameters were TR 8,000 ms; TE 91 ms; matrix 192×192; field of view 240 mm × 240 mm; slice thickness 3 mm. ADC maps were automatically calculated by the vendor specific software on the

[1]Division of Pediatric Radiology, Russell H. Morgan Department of Radiology and Radiological Science, The Johns Hopkins University School of Medicine, Baltimore, MD; [2]Division of Pediatric Neurology, University Children's Hospital, Zurich, Switzerland; [3]Division of Pediatric Oncology, The Sidney Kimmel Comprehensive Cancer Center at Johns Hopkins, The Johns Hopkins University School of Medicine, Baltimore, MD; [4]Division of Pediatric Oncology, University Children's Hospital, Zurich, Switzerland

Grant sponsor: Swiss National Science Foundation; Grant number: PBZHP3-133288; Grant sponsor: Anna Müller Grocholski Foundation, Zurich, Switzerland

Conflict of interest: Nothing to declare.

*Correspondence to: Thierry A.G.M. Huisman, EQNR, FICIS, Professor of Radiology and Pediatrics, Director Pediatric Radiology and Pediatric Neuroradiology, Russell H. Morgan Department of Radiology and Radiological Science, Charlotte R. Bloomberg Children's Center, Sheikh Zayed Tower, Room 4174, 1800 Orleans Street, Baltimore, MD 21287-0842. E-mail: thuisma1@jhmi.edu

Received 28 February 2013; Accepted 5 April 2013

DOI 10.1002/pbc.24578
Published online 12 August 2013 in Wiley Online Library (wileyonlinelibrary.com).

MR scanners. DWI was always performed prior to intravenous contrast injection.

Analysis of the Images

Image analysis was performed on the PACS workstation by an experienced neuroradiologist who was blinded for the tumor histology. A similar methodology to that described by Rumboldt et al. [8] was used (including the calculation of ratios). The solid and enhancing component of the tumor was identified on postcontrast axial T1-weighted images and matching ADC maps. Subsequently, three different regions of interest (ROIs) of 40–100 mm^2 were placed in the solid, non-necrotic, non edematous, enhancing part of the tumors on different MR slices or, if the tumor was small, on the same sections avoiding overlapping. The tumor average ADC values were calculated. Then, one ROI was placed within the normal appearing cerebellar tissue to obtain a control cerebellar ADC value. Two additional ROIs were placed in both thalami. To obtain a second control ADC value, the average thalamic ADC values were calculated. Finally, the ratios of the average ADC tumor values to both the cerebellar and the thalamic control ADC values were calculated.

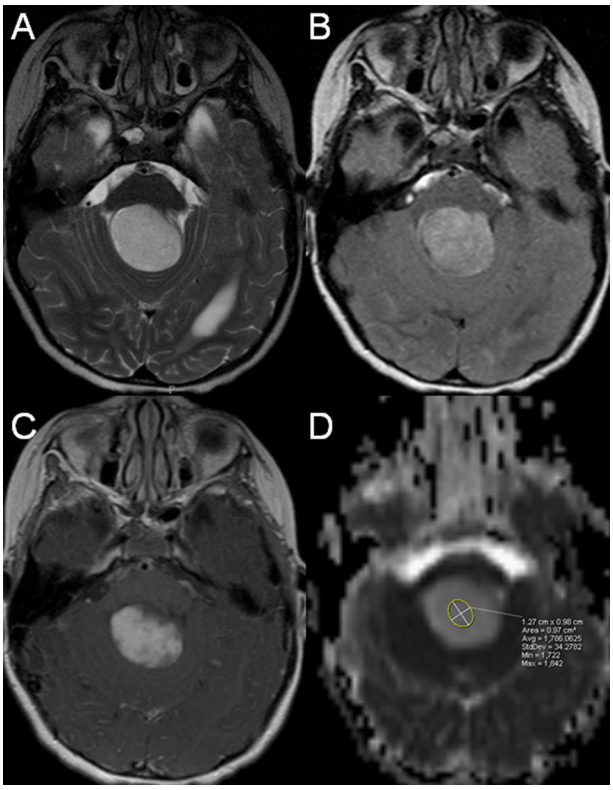

Fig. 1. Eleven-year-old female with cerebellar PA. **A**: Axial T2-weighted and (**B**) FLAIR images show a large, midline mass with heterogenous, hyperintense signal. No surrounding edema is noted. The fourth ventricle is effaced. **C**: axial contrast enhanced T1-weighted image at the same level as (A) and (B) reveal a prominent enhancement. **D**: ADC map corresponding to (A)–(C) reveal matching high ADC-values (hyperintense) compared with normal cerebellar tissue representing increased diffusion.

Histological Findings

The electronic patient records were reviewed for the histological results. On the basis of the neuropathology reports, tumor diagnosis, histological subtype, and WHO grade were recorded for each patient. WHO grade I and II tumors were classified as low-grade tumors, WHO grade III and IV as high-grade. CPP and PA are WHO grade I, all MB histological subtypes and ATRT are WHO grade IV tumors.

Statistical Analysis

Comparison of tumor ADC values and ratios with the tumor grade (low vs. high grade) was done by using a two-sample Mann–Whitney test. Comparison of tumor ADC values and ratios among the most frequent histological types (low-grade astrocytomas, ependymomas, and MBs) was done by using an independent-samples Kruskal–Wallis test. The observed differences were considered as statistically significant if P was less than 0.05.

RESULTS

The inclusion criteria were fulfilled by 24 children (12 females). The median age at pre-surgical MRI was 10 years (range 29 days–18.5 years). Histologic examination revealed ten astrocytomas (42%), nine MBs (38%), three ependymomas (12%), and one ATRT and one CPP of the fourth ventricle, respectively (4%). Astrocytomas included eight PAs (80%, Fig. 1), one WHO grade II astrocytoma, and one glioblastoma multiforme (10%). The histological differentiation of the MB subtypes showed six classic (67%, Fig. 2), two desmoplastic (22%), and one anaplastic MB (11%). Two ependymomas were classified as WHO grade III, one as WHO grade II. Overall, 13 tumors (54%) were classified as high-grade, eleven (46%) as low-grade.

Low- and high-grade tumors could be differentiated by using both absolute ADC values (Fig. 3) and ratios (Figs. 4 and 5). Low-grade tumors showed statistically significantly higher ADC values (1.49 ± 0.25 vs. 0.63 ± 0.18, $P < 0.0001$) and ratios for tumor versus normal cerebellum (2.04 ± 0.33 vs. 0.83 ± 0.25, $P < 0.0001$) and tumor versus thalami (1.98 ± 0.35 vs. 0.79 ± 0.23, $P < 0.0001$; Table I).

Low-grade astrocytomas and MBs could also be differentiated by using both absolute ADC values as well as the tumor/cerebellum and tumor/thalami ratios (Supplementary Table I). Low-grade astrocytomas showed significantly higher ADC values (1.53 ± 0.19 vs. 0.58 ± 0.09, $P < 0.0002$) as well as tumor/cerebellum (2.08 ± 0.27 vs. 0.78 ± 0.12, $P < 0.0002$) and tumor/thalami ratios (2.02 ± 0.28 vs. 0.72 ± 0.12, $P < 0.0002$) compared to MBs. No overlap was found in individual tumor absolute ADC values and ratios between low-grade astrocytomas and MBs. The ADC value and ratios of the patient with glioblastoma multiforme were similar to that of the MB patients.

Ependymomas showed lower ADC values (0.97 ± 0.09 vs. 1.53 ± 0.19, $P > 0.5$) as well as tumor/cerebellum (1.30 ± 0.25 vs. 2.08 ± 0.27, $P > 0.5$) and tumor/thalami ratios (1.24 ± 0.04 vs. 2.02 ± 0.28, $P < 0.5$) compared to low-grade astrocytomas. ADC values (0.97 ± 0.09 vs. 0.58 ± 0.09, $P > 0.5$) as well as tumor/cerebellum (1.30 ± 0.25 vs. 0.78 ± 0.12, $P > 0.5$) and tumor/thalami ratios (1.24 ± 0.04 vs. 0.72 ± 0.12, $P > 0.5$) of ependymomas were higher compared to MBs. There was no overlap between ADC values and ratios of ependymomas and low-grade

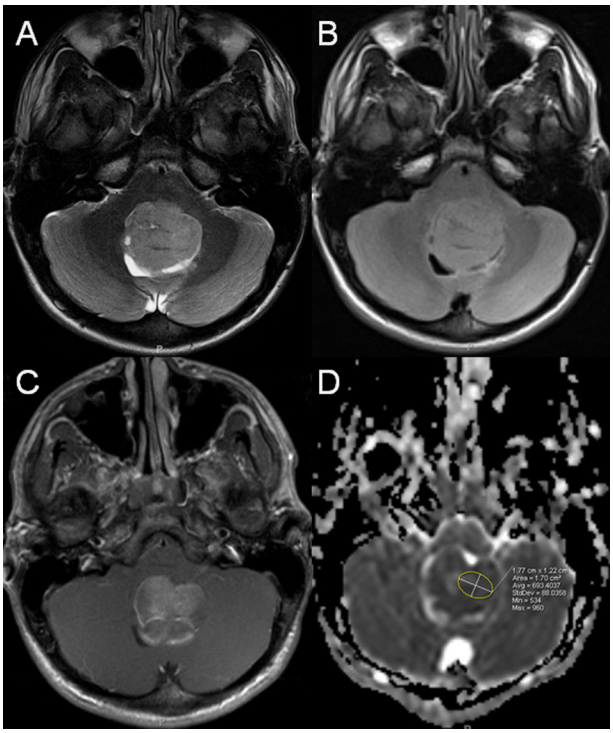

Fig. 2. Fifteen-year-old male with classic MB. **A**: Axial T2-weighted and (**B**) FLAIR images show a large, midline, solid mass with heterogenous, predominantly hyperintense signal. **C**: axial contrast enhanced T1-weighted image at the same level as (A) and (B) demonstrates mild heterogenous enhancement. **D**: ADC map corresponding to (A)–(C) reveal matching low ADC values (hypointense) compared with normal cerebellar tissue representing decreased diffusion.

astrocytomas as well as for MBs and ATRT, respectively. Overlap was found between WHO grade II and III ependymomas for ADC values (0.95 vs. 0.88–1.06) and tumor/cerebellum ratio (1.40 vs. 1.02–1.49), not for tumor/thalami ratio (1.27 vs. 1.20–1.26).

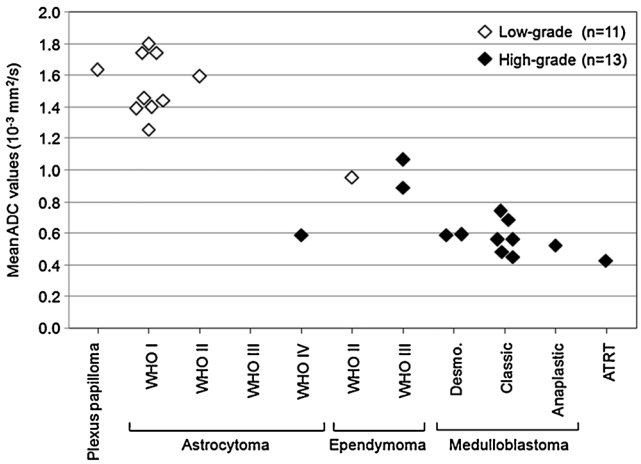

Fig. 3. Scatter diagram of average ADC tumor values for all histologic tumor subtypes; ATRT, atypical teratoid/rhabdoid tumor; Desmo, desmoplastic.

The sensitivity and specificity of a cutoff ADC value of $>1.2 \times 10^{-3}$ mm^2/s for low-grade pediatric cerebellar tumors were 91% and 100%, respectively. The sensitivity and specificity of a cutoff ADC value of $<0.8 \times 10^{-3}$ mm^2/s for high-grade pediatric cerebellar tumors were 85% and 100%, respectively.

DISCUSSION

DWI provides image contrast based on differences in the diffusion characteristics of water molecules within brain tissue. The magnitude of diffusion can be quantified by calculation of the apparent diffusion coefficient (ADC). Diffusion of water molecules within brain tissue is determined by the microstructure in which the diffusion occurs [15]. Accordingly, diffusion is decreased (high intensity on DWI, low ADC values) in densely packed cerebral tissue with high cellularity, small extracellular space, and high nuclear-to-cytoplasmatic ratio. High-grade tumors are typically characterized by a higher cellularity and larger nuclear area than low-grade tumors [16,17]. Decreased diffusion was shown to be characteristic of high-grade tumors and several studies have suggested that analysis of the ADC values may allow for better characterization and grading of pediatric brain tumors non-invasively [7,12].

We are aware of five previous articles that studied the value of DWI in differentiating the various posterior fossa pediatric tumors [7–10,14]. A good correlation between ADC-ratio (tumor vs. normal cerebellar tissue) and histologic classification was shown by Gauvain et al. [7] in five pediatric posterior fossa tumors. Additionally, absolute ADC-values and tumor cellularity/total nuclear area correlated well. Rumboldt et al. [8] showed that the ADC values were significantly higher in PAs than in ependymomas and MBs and ADC values of ependymomas were significantly higher than of MBs in the enhancing solid tumor components of 32 children with cerebellar tumors. However, overlap was found between ADC-values in PAs and ependymomas. ATRT and MBs had similar ADC values. One hundred percent specific ADC cutoff values for PAs ($>1.4 \times 10^3$ mm^2/s) and MBs ($<0.9 \times 10^3$ mm^2/s) were established. Schneider et al. [9] concluded that the ADC values were significantly lower in MBs than in all other tumors in 17 children with untreated posterior fossa tumors. However, an overlap between PAs and ependymomas as well as between ependymomas and MBs was found. The authors concluded that differentiation between PAs and ependymomas as well as ependymomas and MBs by ADC analysis alone was not possible. Jaremko et al. [10] evaluated the ADC maps in 40 children with posterior fossa tumors. They confirmed that diffusion restriction is rare in low-grade tumors and common in high-grade tumors, but they also found an overlap between the measured ADC-values for the different posterior fossa tumors. Finally, Bull et al. [14] attempted to discriminate pediatric brain tumors based on ADC histogram and included 32 posterior fossa tumors. The mean ADC values for PAs were significantly higher compared to ependymomas and no overlap was found between ADC values of PAs and ependymomas/MBs. ADC values for ependymomas were higher than for MBs, but again an overlap was noted. In summary, several studies showed that tumor ADC values may be able to distinguish tumor types and histologic grades. However, overlap of the ADC values for the various tumor types was shown limiting prediction of the tumor grade in individual cases.

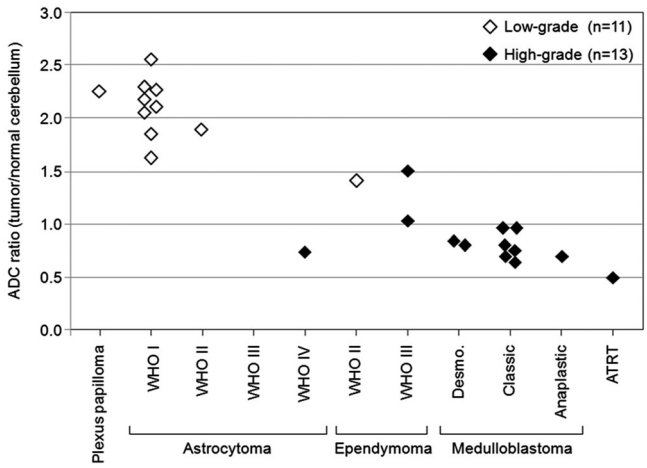

Fig. 4. Scatter diagram of ADC ratios between cerebellar tumors and normal cerebellar tissue for all histologic tumor subtypes; ATRT, atypical teratoid/rhabdoid tumor; Desmo: desmoplastic.

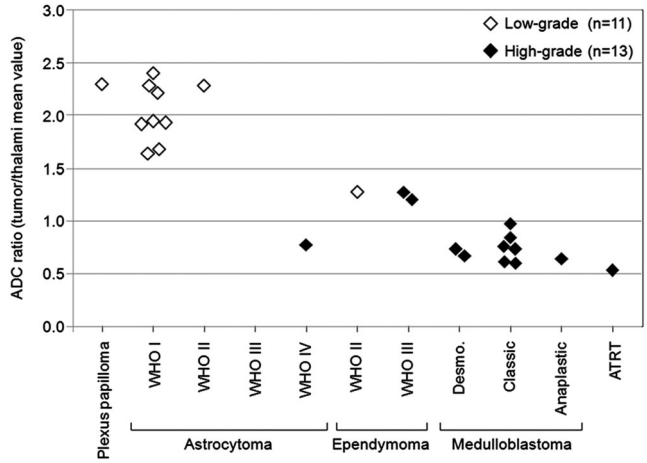

Fig. 5. Scatter diagram of ADC ratios between cerebellar tumors and thalamic tissue for all histologic tumor subtypes. ATRT, atypical teratoid/rhabdoid tumor; Desmo, desmoplastic.

TABLE I. Summary of ADC Values, ADC Ratios of Tumors to Normal-Appearing Cerebellum, and ADC Ratios of Tumors to Thalami for Low-Grade and High Grade Tumors

	Low-grade tumors (n = 11; mean ± SD)	High-grade tumors (n = 13; mean ± SD)	*P*-value
Mean ADC values (10^{-3} mm^2/s)	1.49 ± 0.25	0.63 ± 0.18	$P < 0.0001$
ADC ratio (tumor/normal cerebellum)	2.04 ± 0.33	0.83 ± 0.25	$P < 0.0001$
ADC ratio (tumor/thalami mean value)	1.98 ± 0.35	0.79 ± 0.23	$P < 0.0001$

ADC, apparent diffusion coefficient; SD, standard deviation.

Our study confirms that ADC values are significantly higher in low- than in high-grade tumors. This finding reflects the histological difference between low- and high-grade tumors. High-grade tumors are characterized by high cellularity, low extracellular space, and large nuclear area with high nuclear-to-cytoplasmatic ratio resulting in decreased diffusion and negative correlation between ADC values and tumor grade [7]. Interestingly, in contrast with the previous studies we did not find an overlap for ADC values and ratios between the main histological subgroups of cerebellar tumors (low-grade astrocytomas, ependymomas, and MBs). We explain the absence of overlap in our study design with the rigorous positioning of the ROIs using both pre- and postcontrast T1-weighted and FLAIR images. This approach allowed us to select only solid, non-necrotic, and non edematous tumors' parts for the ROI-based analysis. Indeed, intratumoral necrosis and peritumoral vasogenic edema are associated with high ADC values [18,19]. Inclusion of

necrotic and/or edematous tissue into the ROIs would result in a seemingly elevated ADC value and might explain the previously detected overlap between higher and lower grade tumors. Absence of overlap may also result from the rather small number of patients (total and for every histologic subtype) of our study.

Overlap was however found in our study between ADC values of WHO grade II (low-grade) and WHO grade III (high-grade) anaplastic ependymomas. This finding is similar to that reported by Yamasaki et al. [11]. From a pathologic perspective, this overlap is not surprising. Among ependymomas, the presence of anaplastic features such as high cellularity is notoriously variable in magnitude and extent [20–22]. This variability might have of course a significant impact on the ADC values causing overlap between low- and high-grade ependymomas.

Rumboldt et al. suggested a 100% specific cut off mean ADC value of $>1.4 \times 10^{-3}$ mm^2/s for PAs [8]. This was confirmed recently by Bull et al. [14]. Because of the inclusion of more histological subtypes in our series, an ADC value higher than 1.4×10^{-3} mm^2/s was found not only for PAs, but also for a WHO grade II astrocytoma and a CPP. Based on the same therapeutic approach for these tumors' types, we believe that the former value for PA might be used as a cut off for low-grade cerebellar tumors. To increase its sensitivity, it could be decreased to 1.2×10^{-3} mm^2/s. For MBs, Rumboldt et al. [8] suggested a 100% specific cut off mean ADC values of $<0.9 \times 10^{-3}$ mm^2/s. In our series, an ADC value lower than 0.9×10^{-3} mm^2/s was found not only for all MBs cases, but also for anaplastic ependymomas and a case of ATRT and glioblastoma multiforme, respectively. Because of the overlap between WHO grade II and III ependymomas, we suggest an ADC value lower than 0.8×10^{-3} mm^2/s as 100% specific for high-grade cerebellar tumors.

We used both absolute ADC values and ratios and obtained similar results in agreement with previous studies [8]. Absolute ADC values are easier to measure/calculate and may be the preferred method to differentiate pediatric cerebellar tumors in daily clinical work. Additionally, ADC values of the normal developing brain decrease with increasing age biasing the ADC ratios [8]. ADC ratios, however, are likely less sensitive for differences in scanners, field strengths, and acquisition parameters. ADC ratios may be helpful to compare data between different institutions, for example, in the context of multicentric studies. Additionally, ADC ratios are more likely to correspond to the subjective estimation of the tumor signal characteristics compared to the non-affected cerebellum (e.g., darker, slightly brighter, much brighter), which is the most commonly used evaluation in clinical practice.

DWI and ADC maps have shown to be helpful in the early detection of metastatic diseases or relapsing cerebellar tumors in children. Schubert et al. [23] reported low ADC values in childhood MB with tumor progression or metastatic lesions. The role of DWI and ADC maps in determining postsurgical residual tumor tissue is less clear. On immediate postoperative MRI, Smith et al. [24] demonstrated areas of decreased diffusion adjacent to the resection cavity in 60% of the patients. The DWI-abnormalities resolved in all patients at a median time of 96.5 days (range 8–769 days) following surgery. These DWI-abnormalities are consequently non-neoplastic, but secondary to surgery. Therefore, DWI and ADC maps are not helpful in the first weeks after surgery to distinguish between residual tumor or post-surgical changes.

We are aware of some limitations in our study. The number of patients (total and for every histologic subtype) is rather small preventing statistical analysis for all types of cerebellar tumors and may be avoiding the presence of outliers and, subsequently, overlap in ADC values between tumor types and grades. Additionally, we placed the ROIs in the solid enhancing parts of the tumors. This results in the exclusion of solid, non-enhancing portions of tumors that may bias our results. However, it is highly important to exclude edematous and necrotic parts that would bias the results. The accurate inclusion only of enhancing solid tumor tissue appears a valid approach to achieve this goal. Moreover, our study focused only on one imaging metrics for tumor differentiation. Multiparametric analysis, including data from ^{1}H magnetic resonance spectroscopy and perfusion weighted imaging may further increase the power of predicting cerebellar tumor histology and grade. Larger, prospective, multiparametric and multicentric MRI studies are needed.

In summary, our study shows that assessment of ADC values in enhancing, non necrotic, non edematous, solid parts of cerebellar tumors allows to correctly differentiate high- and low-grade tumors presurgically. Overlap in ADC values was present for WHO grade II and III ependymomas reflecting the heterogeneous histopathological findings. We suggest a 100% specific cutoff ADC value of $>1.2 \times 10^3$ and $<0.8 \times 10^3$ mm^2/s for low- and high-grade pediatric cerebellar tumors, respectively. Careful positioning of the ROIs within the enhancing, non-necrotic, non-edematous, contrast enhancing tumor component appears to be essential.

ACKNOWLEDGMENTS

We are grateful to Prof. Peter Burger, Department of Pathology, Johns Hopkins Hospital, Baltimore, for sharing histological findings, Dr. Ianina Scheer, Department of Diagnostic Imaging, University Children's Hospital, Zurich for her support in collecting neuroimaging data, and Carol B. Thompson, MS MBA, Department of Biostatistics, Johns Hopkins Bloomberg School of Public Health, Baltimore, for her statistical support and expertise. Dr. Poretti was supported financially by the Swiss National Science Foundation (PBZHP3-133288) and the Anna Müller Grocholski Foundation, Zurich, Switzerland.

REFERENCES

1. Howlader N, Noone AM, Krapcho M, et al., editors. SEER Cancer Statistics Review, 1975–2009 (Vintage 2009 Populations). Bethesda: National Cancer Institute. Available at http://seer.cancer.gov/csr/1975_2009_pops09/
2. Pollack IF. Brain tumors in children. N Engl J Med 1994;331:1500–1507.
3. Poretti A, Meoded A, Huisman TA. Neuroimaging of pediatric posterior fossa tumors including review of the literature. J Magn Reson Imaging 2012;35:32–47.
4. Rossi A, Gandolfo C, Morana G, et al. New MR sequences (diffusion, perfusion, spectroscopy) in brain tumours. Pediatr Radiol 2010;40:999–1009.
5. Poussaint TY, Rodriguez D. Advanced neuroimaging of pediatric brain tumors: MR diffusion, MR perfusion, and MR spectroscopy. Neuroimaging Clin North Am 2006;16:169–192.
6. Provenzale JM, Mukundan S, Barboriak DP. Diffusion-weighted and perfusion MR imaging for brain tumor characterization and assessment of treatment response. Radiology 2006;239:632–649.
7. Gauvain KM, McKinstry RC, Mukherjee P, et al. Evaluating pediatric brain tumor cellularity with diffusion-tensor imaging. Am J Roentgenol 2001;177:449–454.
8. Rumboldt Z, Camacho DL, Lake D, et al. Apparent diffusion coefficients for differentiation of cerebellar tumors in children. Am J Neuroradiol 2006;27:1362–1369.
9. Schneider JF, Confort-Gouny S, Viola A, et al. Multiparametric differentiation of posterior fossa tumors in children using diffusion-weighted imaging and short echo-time 1H-MR spectroscopy. J Magn Reson Imaging 2007;26:1390–1398.
10. Jaremko JL, Jans LB, Coleman LT, et al. Value and limitations of diffusion-weighted imaging in grading and diagnosis of pediatric posterior fossa tumors. Am J Neuroradiol 2010;31:1613–1616.
11. Yamasaki F, Kurisu K, Satoh K, et al. Apparent diffusion coefficient of human brain tumors at MR imaging. Radiology 2005;235:985–991.
12. Kan P, Liu JK, Hedlund G, et al. The role of diffusion-weighted magnetic resonance imaging in pediatric brain tumors. Childs Nerv Syst 2006;22:1435–1439.

13. Pillai S, Singhal A, Byrne AT, et al. Diffusion-weighted imaging and pathological correlation in pediatric medulloblastomas—"They are not always restricted!". Childs Nerv Syst 2011;27:1407–1411.
14. Bull JG, Saunders DE, Clark CA. Discrimination of paediatric brain tumours using apparent diffusion coefficient histograms. Eur Radiol 2012;22:447–457.
15. Huisman TA. Diffusion-weighted imaging: Basic concepts and application in cerebral stroke and head trauma. Eur Radiol 2003;13:2283–2297.
16. Kleihues P, Louis DN, Scheithauer BW, et al. The WHO classification of tumors of the nervous system. J Neuropathol Exp Neurol 2002;61:215–259.
17. Thurnher MM. 2007 World Health Organization classification of tumours of the central nervous system. Cancer Imaging 2009;9:S1–S3.
18. Bükte Y, Paksov Y, Genç E, et al. Role of diffusion-weighted MR in differential diagnosis of intracranial cystic lesions. Clin Radiol 2005;60:375–383.
19. Guzman R, Altrichter S, El-Koussy M, et al. Contribution of the apparent diffusion coefficient in perilesional edema for the assessment of brain tumors. J Neuroradiol 2008;35:224–229.
20. Schiffer D, Giordana MT. Prognosis of ependymoma. Childs Nerv Syst 1998;14:357–361.
21. Korshunov A, Golanov A, Sycheva R, et al. The histologic grade is a main prognostic factor for patients with intracranial ependymomas treated in the microneurosurgical era: An analysis of 258 patients. Cancer 2004;100:1230–1237.
22. Ellison DW, Kocak M, Figarella-Branger D, et al. Histopathological grading of pediatric ependymoma: Reproducibility and clinical relevance in European trial cohorts. J Negat Results Biomed 2011;10:7.
23. Schubert MI, Wilke M, Müller-Weihrich S, et al. Diffusion-weighted magnetic resonance imaging of treatment-associated changes in recurrent and residual medulloblastoma: Preliminary observations in three children. Acta Radiol 2006;47:1100–1104.
24. Smith JS, Lin H, Mayo MC, et al. Diffusion-weighted MR imaging abnormalities in pediatric patients with surgically-treated intracranial mass lesions. J Neurooncol 2006;79:203–209.

SUPPORTING INFORMATION

Additional Supporting Information may be found in the online version of this article at the publisher's web-site.

TABLE SI. Summary of ADC Values, ADC Ratios of Tumors to Normal-Appearing Cerebellum, and ADC Ratios of Tumors to Thalami for Low-Grade Astrocytomas and Medulloblastomas.